Optimizing the Monte-Carlo simulation program for NIRS modeling of biological tissues in optoelectronic devices

Wenzheng Wang, Songlin Li, Ibrahim Saliba, Alexandre Hardy, Raphaël Vialle, Julien Denoulet, Sylvain Feruglio

Optimizing the Monte-Carlo simulation program for NIRS modeling of biological tissues in optoelectronic devices

Wenzheng Wang[1], Songlin Li[1], Ibrahim Saliba[1], Alexandre Hardy[2], Raphaël Vialle[3], Julien Denoulet[1], Sylvain Feruglio[1]

[1] *Sorbonne Université, UPMC Université Paris 6, CNRS UMR 7606, LIP6, 75005 Paris, France*
[2] *Département de chirurgie orthopédique, Clinique du Sport Paris, 75005 Paris, France*
[3] *Service de Chirurgie Orthopédique, Hôpital Armand-Trousseau, 75012 Paris, France*

***Abstract*—To support the design of optoelectronic systems using NIRS (Near-Infrared Spectroscopy), we have enhanced and evaluated an open-source software that uses the Monte-Carlo simulation method to model photon propagation in biological tissues. These enhancements enable accurate estimation of the MOP (Mean Optical Path) and penetration depth of incident light, offering researchers tools to simulate and analyze light behavior in biological tissues. We validated these improvements by applying them to both single-layer and multi-layer tissues. The software now features a crucial function to calculate the transmission and reflection rates based on the area and position of the photodetection zone. Validation results indicated that the relative error between the calculated and theoretical transmission and reflection rates was within acceptable limits. These enhancements significantly enhance the software's practicality, aiding researchers in better understanding and utilizing NIRS technology. Thus, simulations of human ankle tissue with the upgraded software confirmed the enhancements' effectiveness through MOP analysis that photons reached the ligament layer.**

***Index Terms*—MCML, Monte-Carlo, MOP, NIRS**

I. Introduction

Optical spectroscopy is a discipline of physics that involves analyzing the electromagnetic spectrum of a more or less complex body over a certain range of wavelengths. It is widely used in both research and industry. In biomedical applications, the visible and near-infrared regions are of growing interest, particularly in the context of embedded health systems [1, 2]. This is often referred to as optoelectronic systems for NIRS (Near-Infrared Spectroscopy) [3].

To date, the development of such systems is still largely empirical [4, 5]. As NIRS is gradually becoming more widely used in medical equipment, knowing only the reflectance and transmittance of different materials is no longer sufficient for specific use cases, such as in fNIRS (functional NIRS) imaging [6], cerebral oximetry monitoring, spinal oximetry, etc. Indeed, it is essential to ensure that the light penetrates through the superficial skin and reaches the target tissue layers in order to obtain accurate information. Therefore, to effectively design a NIRS device tailored to the intended application, it is essential to have an appropriate simulation tool, particularly for modeling the optical path of light and its penetration depth in biological tissues.

In this paper, we begin with a brief introduction of the reference open-source software, MCML, that we used in our study. We then discuss the motivations behind our modifications. An important parameter, the DPF (Differential Pathlength Factor), is used to describe the MOP (Mean Optical Path) and through it, the propagation depth of light. Following the enhancements made to MCML, we conduct three case studies to validate our work. The relevant source codes can be found in [7].

II. Modeling method

A. Presentation of MCML

MCML is an open-source software for steady-state optical simulation in biological media, defined as semi-infinite layered structures [8, 9]. Developed in the 1990s, it has been adapted and enhanced by numerous teams [9–11].

To simulate photon migration in these multilayered media, each light propagation medium must be characterized by four macroscopic optical parameters, defined at a wavelength λ_i:

- μ_a, the absorption coefficient;
- μ_s, the scattering coefficient;
- g, the anisotropy coefficient, with $\mu'_s = (1-g)\mu_s$;
- n, the refractive index.

This stochastic method involves dividing the incident light into photon packets, specified by their weight and position in space. Upon generation, these photons undergo various random events (absorption, scattering, propagation and reflection) that alter their weight and position with each iteration. MCML is capable of performing multiple iterative analyses sequentially for a given wavelength λ_i, thereby simulating the behavior of photons.

The accuracy of the results is proportional to $\frac{1}{\sqrt{N_{ph\_tot}}}$, where N_{ph_tot} the total number of emitted photons, and it is highly dependent on the choice of photon step size during the process. This average free path L_i, between the meshing dimensions of biological tissue, typically ranges from 10 to $1000\mu m$ within NIRS spectrum and is approximated by [9]:

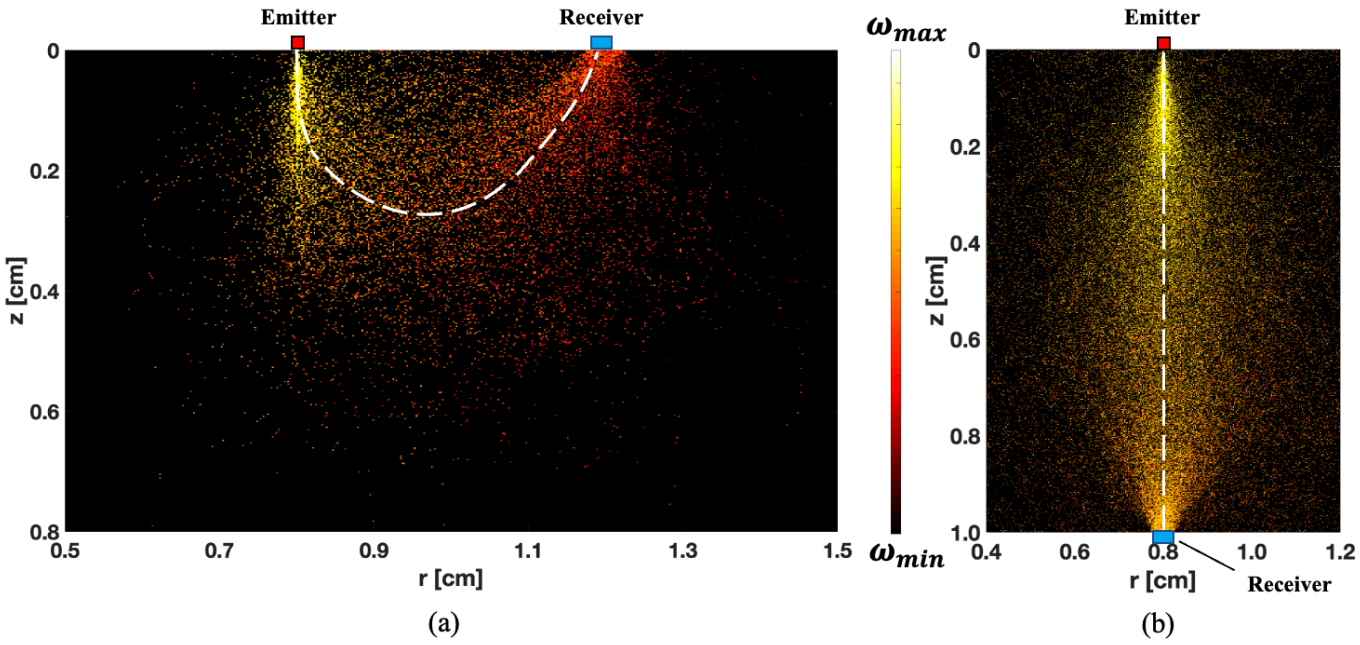

Fig. 1: Distribution of optical paths in reflection (a) and transmission (b) for a layer of human hypodermis

$$L_i = -\frac{ln(\xi_i)}{\mu_a + \mu_s} \tag{1}$$

where ξ is a pseudo-random number with $0 < \xi < 1$.

B. Contributions and additional features to MCML

Before developing a design tool for NIRS systems, we tested software like MCmatlab and Monte-Carlo eXtreme [9, 12, 13]. However, these either failed to display complete photon paths or were too complex to meet our requirements, prompting us to implement specific improvements to MCML.

In its original version, the concept of a photodetection is not included. Therefore, two rectangular photodiodes, adjustable in both position and dimensions, have been added. One detection zone is positioned in the same plane as the emitting source $(z = 0)$ to detect photons reflected by the medium. The other detection zone is placed on the opposite side of the medium $(z = Z_{max})$, capturing photons that pass through the medium. In addition to allowing the source position to be adjustable, we have added the capability for Gaussian and uniform spatial distributions.

The MOP is an important parameter in the modified Beer-Lambert law [4, 14], via the DPF. In practice, this parameter is difficult to obtain and is often used as an adjustment parameter. Therefore, having a more scientifically accurate value is beneficial. It is calculated as the average of the optical paths of all N_{ph} photons received by the photodetector:

$$MOP = \frac{1}{N_{ph}} \sum_{j=1}^{N_{ph}} OP_j \tag{2}$$

where the optical path length for photon j, denoted as OP_j, is calculated as follows [15]:

$$OP_j = \sum_{i=1}^{N} L_i \tag{3}$$

with N, the total number of iterations for one photon.

The photon penetration depth is also a fundamental parameter. It allows for the judicious selection of wavelengths and the definition of the optimal distance between emitter and receiver in reflection mode for a chosen λ_i.

The original version of MCML calculates the reflection factor, R, and the transmission factor, T, over the entire top $(z = 0)$ and bottom $(z = Z_{max})$ surfaces using the following equation:

$$R \text{ or } T = \frac{1}{\omega_i N_{ph\_tot}} \sum_{j=1}^{N_{ph\_X}} \omega_{0j} \tag{4}$$

where:

- ω_i, the initial weight of the photon;
- N_{ph_tot}, the number of photons emitted by the light source;
- ω_{0j}, the weight of the j^{th} photon when it leaves the medium;
- N_{ph_X}, the number of photons exiting from the top of the tissue with $X = R$ or the bottom with $X = T$.

By integrating photodetection into the MCML, we quantified the number of photons received by the photodiodes, allowing us to refine the original calculation method.

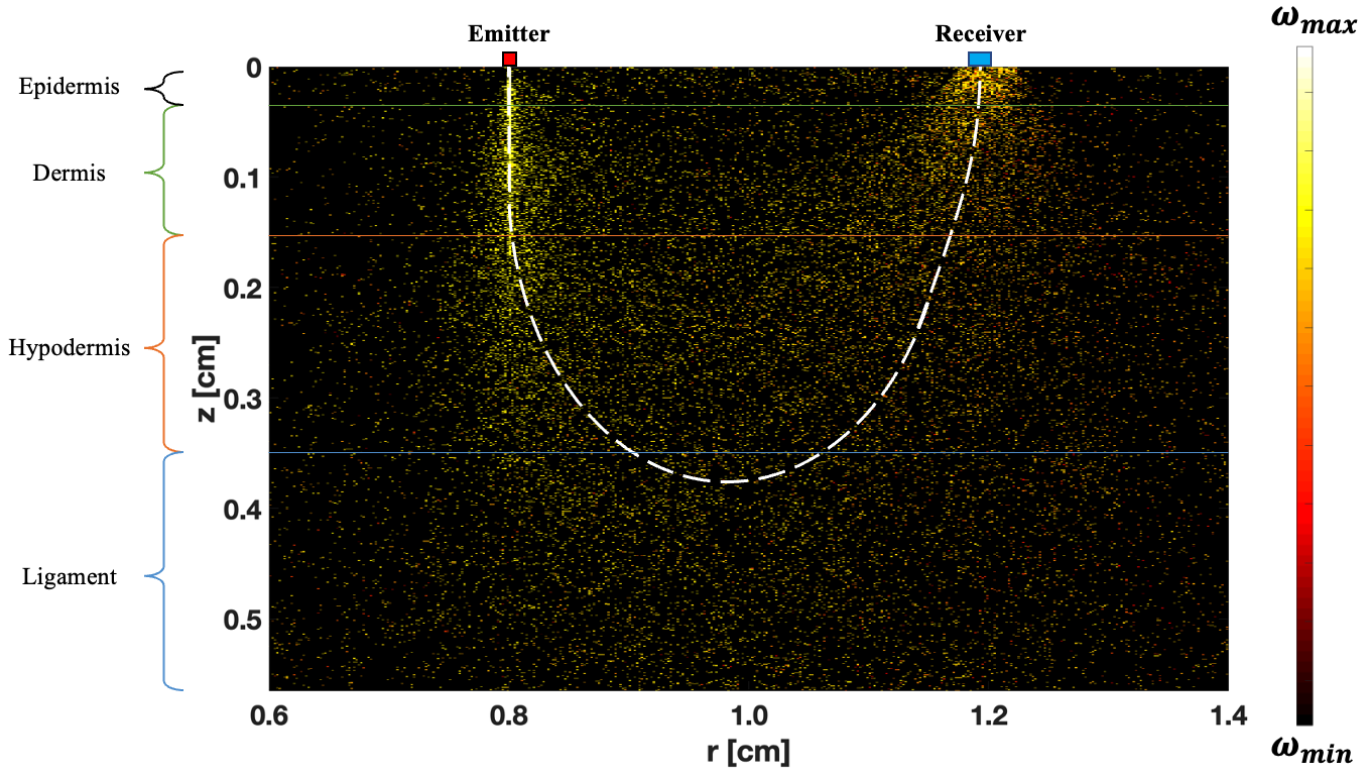

Fig. 2: Simulation results of ankle tissue at $1300nm$

As expressed in equation (5), R and T could be calculated by determining the ratio of the number of photons detected by the photodiode in each mode to the total number of photons.

$$R \text{ or } T = \frac{1}{\omega_i N_{ph\_tot}} \sum_{j=1}^{N_{ph}} \omega_{0j} \tag{5}$$

III. Results and Validation

A. Analysis of a single-layer

Initially, a single layer of human hypodermis with a thickness $Z_{max} = 1cm$ is examined for $\lambda_i = 1300nm$.

We selected this wavelength because the current data on the optical parameters of ligaments at this wavelength is the most comprehensive available, providing a crucial reference for our upcoming experiments [16].

For the simulation, the optical parameters used for this medium one mentioned in Table II, and sourced from [16]. Fig. 1(a) shows the reflection mode simulation results for $N_{ph\_tot} = 2 \times 10^6$ photons and an elementary distance L_i of $10\mu m$. The light source is a point source located at $(x, y, z) = (0.8cm, 0.2cm, 0cm)$. The photodiode, which is a square with a side length of $0.5mm$, is positioned at $(x, y, z) = (1.2cm, 0.2cm, 0cm)$. Fig. 1(b) shows the transmission mode simulation results under the same conditions.

By examining the reflection mode simulation results, we observe that the photons emitted and detected by the photodiode penetrate to a maximum depth of approximately $0.6cm$, with an average penetration depth of around $0.28cm$. The theoretical value, defined by the equation (6) [8], is $0.32cm$, resulting in a relative error of 12.5%.

$$\delta = \frac{1}{\sqrt{3\mu_a(\mu_a + \mu_s(1-g))}} \tag{6}$$

The transmission factor, calculated as follows, gives us a theoretical value of 0.44%, compared to 0.52% in the simulation, resulting in a relative error of 18%.

It is crucial to emphasize that these errors are acceptable within the framework of a Monte-Carlo simulation for a stochastic process, particularly with a high μ_s' [9, 17, 18].

B. Analysis of transmittance in a non-scattering medium

In order to further validate this update, we set the scattering coefficient μ_s of the hypodermis tissue to zero during the simulation, creating an ideal non-scattering medium, and performed several simulations by varying the absorption coefficient μ_a from $0.5cm^{-1}$ to $3cm^{-1}$.

The theoretical value of the transmission coefficient can be calculated using the following equation:

$$T_{th} = e^{-(\mu_a + \mu_s')d} \times 100\% \tag{7}$$

where d represents the tissue thickness.

As shown in Table I, the relative error remained below 5%, indicating satisfactory results for this update.

Absorption coefficient (cm^{-1})	Simulated value (%)	Theoretical value (%)	Relative error (%)
0.5	74.16	77.88	4.78
1.0	57.80	60.65	4.70
1.5	45.12	47.23	4.72
2.0	35.02	36.78	4.79
2.5	27.27	28.65	4.82
3.0	21.30	22.31	4.53

TABLE I: Comparison of simulated and theoretical values

C. Analysis of a multi-layer in reflection

The study object is an ankle, consisting of tissues as defined in Table II [16] with g = 0.9 and n = 1.37 for all elements.

We simulated human ankle tissue under the same reflection mode conditions as previously described, with the results shown in Fig. 2.

The simulation demonstrates that photons emitted from the source reached the ligament tissue and then reflected back to the receiver. At the end of the simulation, it was observed that the photon penetration depth was approximately $0.45cm$, with an optimal distance between the emitter and receiver of $0.4cm$. This allows us to target the ligaments, which are the tissues we aim to assess in the context of ligament repair. The detailed research process can be found in [19].

Layer	**d** (cm)	$\boldsymbol{\mu_a}$ (cm^{-1})	$\boldsymbol{\mu_s}$ (cm^{-1})
Epidermis	0.025	0.71	25.70
Dermis	0.12	1.19	16.20
Hyperdermis	0.20	1.05	15.80
Ligament	0.22	0.70	16.50

TABLE II: Optical parameters of simulated tissues at $1300nm$

IV. Conclusion

Several enhancements have been made to the reference software MCML, resulting in a robust simulation tool for designing the optoelectronic components of NIRS systems. This tool facilitates the optimization of wavelength selection and the positioning of optical emitters and receivers based on the tissues to be monitored. Estimating MOP is also a crucial aspect for applying the modified Beer-Lambert law.

Improvements are being made in an ongoing project, with automatic identification of MOP in tissues and envelopment of propagation paths, as well as a useful GUI (Graphical User Interface) to be added to the final version. These enhancements will allow for the calculation of light propagation depth in biological tissues using advanced algorithms, providing significant reference value for actual measurements. Additionally, efforts will be made to accelerate the simulation process, which is currently not optimized, with the ultimate goal of integrating the tool into a co-design environment.

V. Acknowledgment

The authors are thankful to IUIS (*Institut Universitaire d'Ingénierie en Santé*) for funding this project.

References

[1] A.F. Ferreira, H.P. da Silva, H. Alves, N. Marques, A. Fred. Feasibility of Electrodermal Activity and Photoplethysmography Data Acquisition at the Foot Using a Sock Form Factor. Sensors 2023, 23, 620. DOI: 10.3390/s23020620.

[2] M.G. Joo, D.H. Lim, K.K. Park, J. Baek, J.M. Choi, H.W. Baac. Reflection-Boosted Wearable Ring-Type Pulse Oximeters for SpO2 Measurement with High Sensitivity and Low Power Consumption. Biosensors 2023. DOI: 10.3390/bios13070711.

[3] M. Ferrari, V. Quaresima. A brief review on the history of human functional near-infrared spectroscopy (fNIRS) development and fields of application. NeuroImage, 63(2), 921-935. DOI: 10.1016/j.neuroimage.2012.03.049.

[4] N. Mainard, O. Tsiakaka, S. Li, J. Denoulet, K. Messaoudene, R. Vialle, S. Feruglio. Intraoperative Optical Monitoring of Spinal Cord Hemodynamics Using Multiwavelength Imaging System. Sensors 2022, 22, 3840. DOI: 10.3390/s22103840.

[5] O. Tsiakaka, B. Gosselin, S. Feruglio. Source-Detector Spectral Pairing-Related Inaccuracies in Pulse Oximetry: Evaluation of the Wavelength Shift. Sensors 2020. DOI: 10.3390/s20113302.

[6] V. Quaresima, M. Ferrari. A Mini-Review on Functional Near-Infrared Spectroscopy (fNIRS): Where Do We Stand, and Where Should We Go? DOI: 10.3390/photonics6030087.

[7] Source code available in the Gitlab of LIP6. https://gitlab.lip6.fr/feruglio/mop-mcml.git.

[8] S.L. Jacques. (2022). History of Monte Carlo modeling of light transport in tissues using mcml.c. Journal of biomedical optics, 27(8), 083002. DOI: 10.1117/1.JBO.27.8.083002.

[9] Monte-Carlo scattering program. https://omlc.org/software/mc/.

[10] S. Chatterjee, P.A. Kyriacou. Monte Carlo Analysis of Optical Interactions in Reflectance and Transmittance Finger Photoplethysmography. Sensors 2019. DOI: 10.3390/s19040789.

[11] E. Sarmiento-Gómez, B. Morales-Cruzado. "GA-GPU-MCML: A New GPU Accelerated Algorithm for Optical Properties Recovery," in Biomedical Optics 2016, OSA Technical Digest (Optica Publishing Group, 2016), paper JTu3A.13. DOI: 10.1364/CANCER.2016.JTu3A.13.

[12] MCmatlab user guide. https://github.com/ankrh/MCmatlab.

[13] Monte Carlo eXtreme. Physically accurate and validated GPU ray-tracer. https://mcx.space.

[14] S. Li. Modélisation d'un implant médical intelligent dans son environnement pour le monitorage fonctionnel de la moelle épinière. Ingénierie biomédicale. Sorbonne Université, 2022. Français. https://theses.hal.science/tel-04028226.

[15] S. Chatterjee, J.P. Phillips, P.A. Kyriacou. Monte Carlo investigation of the effect of blood volume and oxygen saturation on optical path in reflectance pulse oximetry[J]. Biomedical Physics and Engineering Express, 2016, 2(6): 065018. DOI: 10.1088/2057-1976/2/6/065018.

[16] A.N. Bashkatov, E.A. Genina, V.V. Tuchin. Optical properties of skin, subcutaneous, and muscle tissues: a review[J]. Journal of innovative optical health sciences, 2011, 4(01): 9-38. DOI: 10.1142/S1793545811001319.

[17] M. Parsanasab, C. Hayakawa, J. Spanier, Y. Shen, V. Venugopalan. Analysis of relative error in perturbation Monte Carlo simulations of radiative transport. Journal of biomedical optics, 2023. DOI: 10.1117/1.JBO.28.6.065001.

[18] J.Y. Lee, S. Ahn, S.H. Nam. (2022). Performance estimation of optical skin probe in short wavelength infrared spectroscopy based on Monte-Carlo simulation. Scientific reports, 12(1), 20134. DOI: 10.1038/s41598-022-23251-4.

[19] I. Saliba, A. Hardy, W. Wang, R. Vialle, S. Feruglio. A Review of Chronic Lateral Ankle Instability and Emerging Alternative Outcome Monitoring Tools in Patients following Ankle Ligament Reconstruction Surgery. J. Clin. Med. 2024, 13, 442. DOI: 10.3390/jcm13020442.